Hindawi
Advances in Civil Engineering
Volume 2020, Article ID 8838179, 18 pages
https://doi.org/10.1155/2020/8838179

Research Article

Improving the Interfacial Bond Properties of the Carbon Fiber Coated with a Nano-SiO_2 Particle in a Cement Paste Matrix

Gwang-Hee Heo,[1] **Jong-Gun Park**,[2] **Ki-Chang Song**,[3] **Jong-Ho Park**,[3] **and Hyung-Min Jun**[4]

[1]*Department of International Civil and Plant Engineering, Konyang University, 121 Daehak-Ro, Nonsan-Si, Chungnam-Do, Republic of Korea*
[2]*Public Safety Research Center (PSRC), Konyang University, 121 Dachak-Ro, Nonsan-Si, Chungnki-Changam-Do, Republic of Korea*
[3]*Department of Biomedical Materials, Konyang University, 158 Gwanjedong-Ro, Seo-Gu, Daejeon Metropolitan-Si, Republic of Korea*
[4]*Department of Disaster and Safety Engineering, Konyang University, 121 Dachak-Ro, Nonsan- Si, Chungnam-Do, Republic of Korea*

Correspondence should be addressed to Jong-Gun Park; 2630@hanmail.net

Received 1 June 2020; Revised 27 July 2020; Accepted 16 September 2020; Published 29 September 2020

Academic Editor: Zhongguo John Ma

To improve the interfacial bond properties of the carbon fiber coated with a nano-SiO_2 particle in a cement paste matrix, the present study proposed a method of coating nano-SiO_2 particles on the surface of the carbon fiber by the chemical reaction of a silane coupling agent (glycidoxypropyltrimethoxysilane, GPTMS) and colloidal nano-SiO_2 sol in an alkaline environment. To verify whether a nano-SiO_2 particle was effectively modified on the surface of the carbon fiber, the surface morphology, chemical composition, and chemical structure were characterized and analyzed by several techniques such as the scanning electron microscope (SEM), energy-dispersive spectrometer (EDS), and Fourier-transform infrared spectroscopy (FT-IR). Nano-SiO_2 particles were entirely covered and uniformly distributed on the surface of the carbon fiber, resulting in the formation of a thin layer of nano-SiO_2 particles. A thin layer of nano-SiO_2 particles reacted with $Ca(OH)_2$ to form a calcium-silicate-hydrate (C-S-H) gel, which is most helpful to increase the form between the fiber and the matrix. In addition, a pull-out test of the tow carbon fibers was performed to verify the effect of the new surface modification method on the interfacial bond properties of the carbon fiber embedded in the cement paste matrix. The experimental results showed that the frictional bond strength of the carbon fiber coated with a nano-SiO_2 particle was significantly increased compared to the plain carbon fiber. These results were expected to improve the interfacial bonding force of hardened cement paste from the formation of the C-S-H gel produced through the chemical reaction of nano-SiO_2 particles coated on the surface of the carbon fiber with $Ca(OH)_2$. In particular, it was confirmed that the carbon fiber-reinforced cement paste (CFRCP) specimens coated with a nano-SiO_2 particle and silica fume which replaced 10 wt.% of cement by mass showed the highest pull-out resistance performance at 28 days of age. The new surface modification method developed in this study can be very beneficial and helpful in improving the interfacial bond properties of CFRCP.

1. Introduction

Around the world, cement-based composites are indispensable to the technological development of modern civil engineering and have been widely used in architectures and infrastructure facilities [1–4]. Cement-based composites have high compressive strength, but lower tensile, flexural, and impact strengths, as well as such faults as brittle properties [5–7]. In order to prevent sudden brittle fracture like this, research studies on fiber-reinforced cement composites (FRCC) have been conducted continuously, and various types of fibers are widely applied to the construction

of civil engineering materials. For this reason, addition of suitable fibers is required to improve the performance of cement-based composites [8–11].Incorporating of fibers into a cement composite material can inhibit cracking and growth due to the bridging action of the fibers and increase ductility in tension and compression, as well as provide safety performances such as dynamic loading, impact, and explosion [12–14].

Currently, the types of fibers used in FRCC are steel, carbon, glass, polyvinyl alcohol (PVA), polypropylene (PP), polyethylene (PE), asbestos, cellulose, and so on. Among these fibers, steel fiber as cement reinforcing materials has been widely used for constructing infrastructures or facilities such as road pavement, tunnels, bridges, and dams and has excellent mechanical performance with high tensile strength and ductility [4, 15–17]. Meanwhile, carbon fiber has light weight, high strength, high modulus, and excellent corrosion resistance. Because of this, it is used most frequently in the aerospace industry in recent years and has been rapidly attracting attention in many industries, such as energy, sports, and leisure, mechanical structures, electric vehicles, and civil and constructions [18, 19]. In particular, carbon fiber as a fiber-reinforced cement composite is expected to gradually increase its application in various construction industries such as building materials, concrete structures, seismic reinforcement, repair and reinforcement of bridges, tunnel reinforcement materials, agricultural repair structures, and super heat-resistant applications. Moreover, the bond properties between the fibers and the matrix play an important role in the mechanical properties of the composites [20, 21]. If the bond strength between the fiber and the cement matrix is sufficient, it is very advantageous to prevent the fiber from pull-out or fracture in the matrix when cracking occurs. Unless the bond strength is sufficient, the advantages of high elasticity and high strength owned by the fiber cannot be sufficiently exhibited. For this reason, many studies have been conducted to increase the bond strength between the fibers and the matrix in the cement paste matrix, thereby increasing the fiber enhancement effect, and to improve the mechanical properties of the cement composite material [22–25].

However, in the previous domestic and foreign studies, research studies have been conducted steadily to investigate the interfacial bond properties of FRCC using carbon fibers, but there are in fact not many research studies conducted yet to manufacture the carbon fiber and develop CFRC (carbon fiber-reinforced cement) composites with improved bond performance by increasing the interfacial bonding force between the fibers and the matrix. Besides, the information about various research results on the interfacial bond properties of the carbon fiber in the cement paste matrix is quite insufficient. In Korea, the research data specifically of the interfacial bond properties between the fibers and the cement matrix are extremely limited [26]. It is necessary to develop a surface sizing treatment of the carbon fibers in order to improve the interfacial bonding force between the fibers and the matrix. In particular, the surface of the carbon fiber is very smooth and clean, so it is difficult to form a cement hydrate product between the fibers due to low hydrophilicity. In addition, carbon fiber may have a problem that the interfacial adhesion between the fiber and the matrix is weak due to the nonhydrophilic material on the fiber surface. In order to improve this problem, sizing treatment of the carbon fibers is performed to improve the interfacial bonding force between the fibers and the matrix. The surface sizing treatment has been reported to coat carbon fibers with sizing to chemically bond the surface of fibers to the matrix, thus creating a more stable physical interface [27–29].

Recently, several methods for improving the pull-out resistance performance of fibers have been introduced and are mainly focused on steel fibers. Steel fiber can be made into a special shape, improving the mechanical properties between the fiber and the matrix [30–33]. Adding an expansion agent to the cement-based composite material is expected to increase the synergistic effect since it causes an interaction between the fibers and the cement matrix in the compression state. Silica fume and nano-SiO_2 were added to increase the bond strength of the steel fiber in cement composites [7, 34–38]. As a flexible fiber, thin carbon fiber is hard to shape; thus, the method of surface modification should be the suggested approach. Oxidation treatment is an effective method to improve the flexural performance (flexural strength or toughness) of CFRCP [29, 39, 40]. In order to apply the carbon fiber as a cement reinforcing material, it is very important to improve the interfacial bonding force between the fiber and the matrix. A recent study proposed a surface modification method to increase the bond strength of the carbon fiber coated with a thin layer of nano-SiO_2 particles in the cement paste matrix [41]. Carbon fiber coated with a nano-SiO_2 particle reacts with $Ca(OH)_2$, a cement hydration product, to play a decisive role in improving the interfacial bonding force. This method has the disadvantage that the pretreating process of the carbon fiber with a silane coupling agent is very complex and takes a lot of time before coating the surface of the carbon fiber with a nano-SiO_2 particle in the cement paste matrix. Thus, this study is different from the conventional method of coating the surface of the carbon fiber with silica sol (ss-sol) after pretreating the fiber with a silane coupling agent to improve the interfacial adhesion of the carbon fiber; the process is simplified by a new surface modification method in which synthetic obtained by the reaction of a silane coupling agent with silica sol is coated directly on the surface of the carbon fiber. This study aims to provide a method for manufacturing carbon fibers coated with a nano-SiO_2 particle and develop CFRCP to improve the interfacial bonding force of carbon fibers in a cement paste matrix.

Therefore, this study proposed a new surface modification method to directly coat on the surface of the carbon fiber using silica sol (ss-sol) after pretreating the fiber with GPTMS to improve the interfacial bond properties between the fiber and the matrix. It is expected that the coated nano-SiO_2 particles react with $Ca(OH)_2$, a cement hydration product, to improve interfacial adhesion. To determine whether nano-SiO_2 particles are effectively bonded to the surface of the carbon fiber during this process, we analyzed and observed the surface morphology, chemical composition, and chemical structure using SEM, EDS, and FT-IR of

hardened CFRCP. The chemical reaction process and the degree of chemical reactivity of the modified surface were then determined. In addition, pull-out tests at 3, 7, and 28 days of age were performed to confirm the effect of the surface modification method on the frictional bond strength of the carbon fibers in the cement paste matrix. From the stress-displacement relationship curve obtained by the pull-out test, the frictional bond strength for the CFRCP specimens with the coating of carbon fibers and with or without silica fume was compared and analyzed, and tow pull-out resistance performance of carbon fibers was reviewed. After the pull-out test, the fractured surface of the CFRCP specimens was observed and analyzed through SEM imaging.

2. Materials and Experimental Methods

2.1. Surface Modification of the Carbon Fiber

2.1.1. Reagents and Materials. The reagents and materials used in this study are colloidal silica sol (ss-sol 30a, 30 wt.%, S-Chemtech Co., Ltd.) in which nano-SiO_2 particles having a size of 10 nm are dispersed, and nitric acid (HNO_3, 60 wt.%, Samchun Chemical) is used as a catalyst. The reagents and materials used for the experiment are GPTMS (99.9%, Sigma-Aldrich) as a silane coupling agent, ethylenediamine (EDA, 99.9%, Sigma-Aldrich) as a hardener, and ethanol (EtOH, 99.0%, Samchun Chemical) as a solvent. Reagents were applied without purification and chemical treatment process. Figure 1 is a photograph of the tow carbon fiber used in the experiment.

Figure 1: Appearance of the tow carbon fiber.

2.1.2. Surface Modification Method. In the manufacturing process of the nano-SiO_2 coating solution, 3.6 g of GPTMS was uniformly mixed in 150 ml ethanol and 150 ml distilled water, and nitric acid was added to adjust pH of the solution to 2. Then, the pH-adjusted solution was stirred at 70°C for 12 hours, and 445.5 g of colloidal nano-SiO_2 sol was added to the solution to react at 70°C for 24 hours. Finally, for the purpose of ring opening of the GPTMS epoxy group, 0.54 g of EDA, a hardening agent, was added dropwise and further stirred at 40°C for 2 hours to finally prepare nano-SiO_2 coating solution. Here, ring opening generally means that the ring of the cyclic compound is opened to form a linear polymer. Nano-SiO_2 sol is effective in uniformly synthesizing high-purity nano-SiO_2 particles at low temperatures. This study was used to coat nano-SiO_2 particles on the surface of the carbon fiber and to investigate the reactivity between nano-SiO_2 particles coated on the surface of the carbon fiber. The reinforcing mechanism of the surface-modified carbon fiber is known to motivate the nano-SiO_2 particles generated on the surface of the carbon fiber to react with the hydration product $Ca(OH)_2$ in the cement paste matrix and to form a C-S-H gel, thus improving the interfacial bonding force between the fiber and the matrix. Therefore, the success of this study is essential for the reactivity between $Ca(OH)_2$ and nano-SiO_2 particles coated on the surface of the carbon fiber. Figure 2 is a diagram schematically showing the surface modification process of the carbon fiber. First, all impurities attached to the carbon fiber were removed using acetone, the carbon fiber was oxidized by soaking it in nitric acid solution for 24 hours to increase its surface activity, and the oxidized carbon fiber was washed with distilled water and dried at 110°C in an oven. Then, the dried carbon fiber was modified to be hydrophilic by attaching nano-SiO_2 particles to its surface following the process of soaking in the hydrophilic silica coating solution synthesized through the above process for 3 hours. Here, hydrophilic generally refers to the property of easily bonding to water molecules. After curing in an oven at 80°C for 1 hour, it was washed again in distilled water and dried at 120°C for 2 hours to prepare a final carbon fiber.

2.2. Experimental Methods

2.2.1. SEM for Surface Morphology Observation. In this study, SEM images were taken to check whether nano-SiO_2 particles were uniformly dispersed on the surface of the carbon fiber. In addition, the fibers obtained by crushing the produced CFRCP specimens were dried, and then the size of uncoated and coated carbon fibers was measured by SEM imaging. As the analysis equipment, MIRA LMH high-resolution SEM model of TESCAN was used. The analysis was performed at 10 kV (ACC voltage), and after the sample was coated with platinum under Ar gas, it was observed to check whether nano-SiO_2 particles were attached to the surface of the carbon fiber.

2.2.2. EDS for Chemical Element Analysis. EDS is a device that is additionally attached to the SEM equipment and collects specific X-rays generated by the electron beam of the SEM to analyze the chemical composition of the specimen. When the electron beam is shot to a point or area of a specimen, it is elated by the energy of the atom. At this time, the intrinsic energy emitting specific X-ray is different for each material, and this value is used to analyze the chemical composition of the material. In this study, for quantitative chemical analysis of the surface of the carbon fiber, the composition was carried out with an EDS detector of Bruker Co. through SEM. EDS is also frequently used for cement-based materials in combination with SEM. The relative

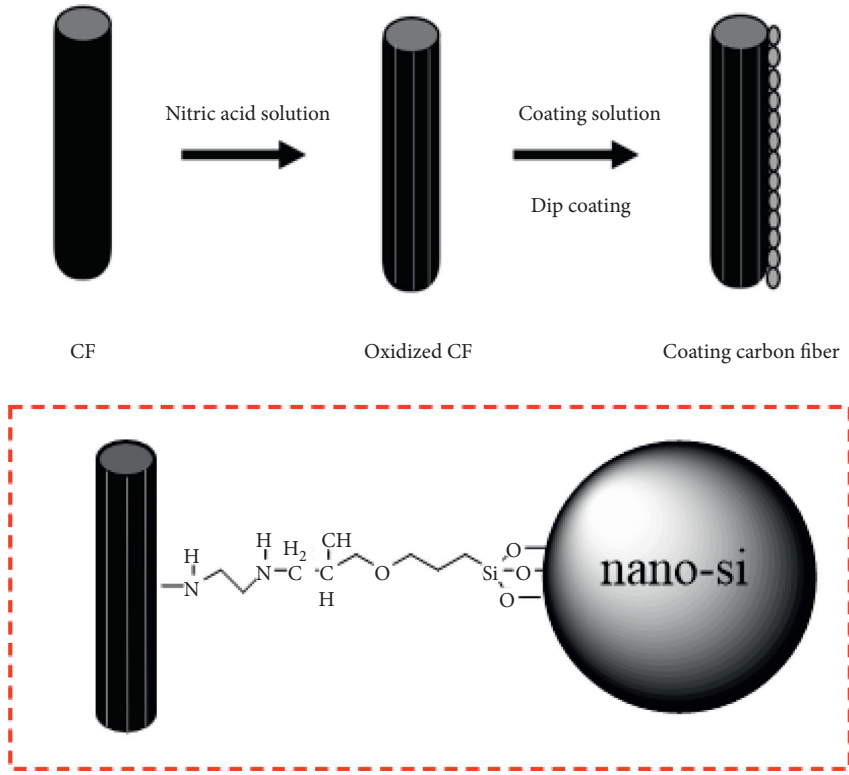

Figure 2: Surface modification process of the carbon fiber.

contents of C, O, Si, and Ca around the fiber were measured using the EDS area scanning method as well as the spot-analysis method. In order to accurately determine the content of chemical components that are hydration products, the content of chemical components was measured by obtaining the average values at 5 points in the same specimen.

2.2.3. FT-IR for Chemical Structure Determination. A specific chemical bond or functional group has a specific absorption frequency for infrared light. FT-IR detects the presence of a specific chemical bond or functional group to determine whether a specific substance is present. In addition, FT-IR is frequently used with cement-based materials for the detection of cement clinker and hydrated products. In the test, attempts were made to use FT-IR (produced by Cary 630, Agilent Technologies) which can measure the wavelength in the range of 4000–400 cm^{-1} to determine whether nano-SiO_2 particles were chemically attached to the surface of the carbon fiber in an effort to confirm if C-S-H gel with hydrated cement particles is present on the surface of the carbon fiber coated with a nano-SiO2 particle.

2.2.4. Pull-Out Test. This study was carried out in accordance with the test methods of ASTM D 4018 [42] and ASTM D 3039/D 3039M [43] in order to review the pull-out resistance performance of tow carbon fibers embedded in a cement paste matrix. Figure 3 shows the specimen installation and experimental setup for the tow carbon fiber pull-out test. A jig was attached to a load cell having a capacity of 100 kN to measure the pull-out load and displacement using a noncontacting dynamic strain analysis system (NCDSAS, Intron Co., Ltd.). During the test, the pull-out speed was constantly controlled to a displacement of about 2.0 mm/min. The pull-out property data were automatically measured by a load cell installed inside the NCDSAS. To fix the specimen, the tow carbon fiber was tied up by connecting the upper moving end and lower fixing end of the pull-out test device to the jig grip and attaching using a double-sided tape. At this time, it was reinforced with a paper of about 0.3 mm thick to prevent slip of the grip surface and the specimen. When the maximum load of the fiber is reached during the pull-out test, the maximum pull-out load is calculated by dividing the total surface length of the fiber by the specific surface area. The frictional bond strength at the maximum load on the interface is calculated by the following formula:

$$\tau_{\max} = \frac{P_{\max}}{\pi\, DL}, \tag{1}$$

where $\tau_{\max}$ is the bond strength of the embedded fibers based on the maximum pull-out load (MPa), $P_{\max}$ is the maximum pull-out load (N), D is the diameter of the fiber (mm), and L is the embedded length of the fiber (mm).

2.2.5. Pull-Out Load-Displacement Curve. Figure 4 shows a schematic of typical pull-out load-displacement curves and associated post-pull-out mechanisms studied by Kanda and Li [44] and Naik et al. [32]. In Figure 4, it has been shown that the pull-out load increases due to the bond force between the fiber and the matrix, and after the maximum bond

Figure 3: Specimen installation and experimental setup for the pull-out test of the tow carbon fiber.

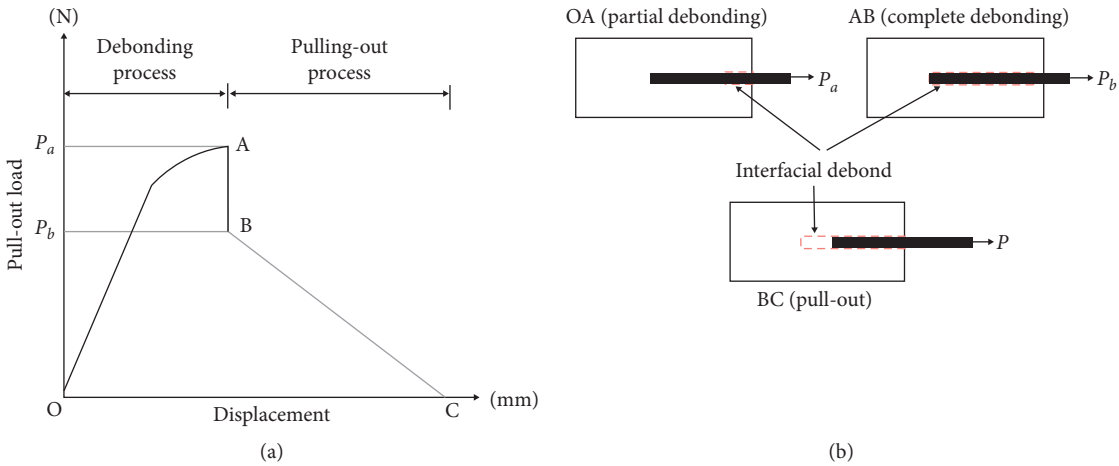

Figure 4: Schematic of typical pull-out load-displacement curves and associated post-pull-out mechanisms.

load is exceeded, it is converted into a pull-out behavior from the cement matrix. Generally, two different parts can be distinguished from the load-displacement curve obtained during the pull-out test of FRCC. In the first part, displacement increases almost linearly in the range where the pull-out load is small; and then, as the pull-out load increases, displacement increases with gentle slope, and then the maximum pull-out load is reached. This process is called the debonding area. The first cracking region is the moment when cracking occurs, and before that moment, the pull-out load-displacement curve is linear. In the second part, after reaching the maximum pull-out load and passing inflection point A, the curve is directed toward point B, and when the fiber is fractured or debonded, the pull-out sudden load drop occurs. Even after fracture or debonding of the fiber, it shows a convergence form, falling from point B to point C. This process is called the debonding area. This is the postcracking area where fibers are completely pulled out, and then the pull-out load-displacement curve is shown gently sloped. In general, when fibers are pulled out, the stress acting within fibers is lower than the yield stress, and when a good number of fibers are mixed and the pull-out does not occur, the fracture of the fibers occurs due to some separation. Therefore, when a crack occurs in the cement matrix, the stress is transferred to the fiber as crack propagates, and the maximum pull-out load is determined by gradual separation.

2.2.6. Calculation of the Nominal Diameter of the Carbon Fiber. To calculate the nominal diameter of the tow carbon fiber, the nominal diameter of the fiber is obtained from formula (2) where the cross section of the fiber is divided by π to get the square root according to KS F 2564 (steel fiber for concrete) [45]:

$$d_n = 2\sqrt{\frac{A}{\pi}}, \quad (2)$$

where d_n is the nominal diameter (mm) and A is the cross-section area of the fiber (mm^2).

2.2.7. Compressive Strength Test. The compressive strength test of the cement paste was carried out according to the test method of KS L ISO 679 [46]. The specimen for this test was prepared at the same size ($40 \times 40 \times 40$ mm) as that of the pull-out test. It was demolded after 24 hours, and the dried specimen was cured at $20 \pm 2^{\circ}C$. For the specimens that had been cured, the compressive strength was measured at 28 days of age using a universal material tester (MTDI Co., Ltd., Korea). In the compressive strength test, the loading area was 1,600 mm^2, and the loading speed was applied at a constant speed under the condition of 2400 N/s. The compressive strength of the cement paste can be calculated from the following formula:

$$f_c = \frac{P}{bh}, \quad (3)$$

where f_c is the compressive strength (MPa), P is the maximum load (N) obtained from the test, b is the width (mm) of the specimen, and h is the height (mm) of the specimen.

2.3. Preparation of the Specimen

2.3.1. Cement and Silica Fume. The cement used in this study was ordinary Portland cement (OPC) type I produced by S company in Korea specified in KS L 5201, the specific gravity was 3.13, and the grade of the powder was 3,860 cm^2/g. Besides, silica fume is Norwegian microsilica having an average particle size of 0.15 μm (particles exceeding 45 μm are 0.1% or less). The specific surface area is 200,000 cm^2/g, and it is an ultrafine powder silica product. The physical properties and chemical compositions of cement and silica fume are shown in Table 1.

2.3.2. Carbon Fiber. The PAN-based (polyacrylonitrile) high-strength carbon fibers (T700SC-12000) used in this experiment were manufactured and produced by T company in Japan, and they have a tensile strength of 4,900 MPa and an elastic modulus of 230 GPa. The material properties of the carbon fiber are shown in Table 2. Figure 5 is a photograph showing the shapes of the plain carbon fiber and nano-SiO_2-coated carbon fiber used in the experiment.

2.3.3. Preparation of Cement Pastes. For the composites and workability of the cement pastes, cement and water only were used, and the aggregates (sand and gravel) and admixture were not used. At this time, the water-binder ratio (w/b) was 0.4, and silica fume replaced 10 wt.% of cement by mass. The binder-to-water ratio was 1 : 0.4. For mixing cement paste, a mechanical mixer (Jeil Precision Co., Ltd., South Korea, JI-206) was used. It was carried out according to the test method of KS L 5109-2017 for "practice for mechanical mixing of hydraulic cement pastes and mortars of plastic consistency." As for the mixing method, first, the whole amount of blended water is poured into the mixing container. The cement is then put in water and left for 30 seconds to absorb water. The mixer was then operated to mix for 30 seconds at low speed. Then, the mixer was stopped, and all cement pastes were scraped off for 15 seconds. Finally, the mixer was operated again to mix for 60 seconds at high speed. The total mixing time was about 2 minutes. After filling the mixed cement paste with a $40 \times 40 \times 40$ mm cubic mold, it was tamped sufficiently using a compaction rod or shaking by hands and then finished again with a trowel. In addition, in order to perform proper curing of the cement pastes, they were wrapped with a plastic sheet (vinyl) for 24 hours before demolding to suppress rapid evaporation of moisture. After mold demolding, they were air-dried at 3, 7, and 28 days of age, respectively, at the room temperature of about $20 \pm 2^{\circ}C$.

Table 1: Physical and chemical properties of cement and silica fume.

Materials	OPC	Silica fume
Specific gravity	3.13	2.2
Surface area (cm^2/g)	3,870	200,000
SiO_2 (%)	21.47	97.38
Al_2O_3 (%)	6.21	—
Fe_2O_3 (%)	3.70	—
CaO (%)	59.24	—
MgO (%)	2.08	—
Na_2O (%)	0.13	0.11
K_2O (%)	1.08	0.31
SO_3 (%)	2.48	—
Loss on ignition (%)	2.87	0.67
F-CaO (%)	0.57	—
H_2O (%)	—	0.57

2.3.4. Fabrication of Specimens. A description of fabrication of specimens for the pull-out test is shown in Table 3. Figure 6 shows the production progress of each step for the specimen fabrication of the carbon fiber embedded in the cement paste matrix. As shown in Figure 6, a special type of wooden mold was made and divided into Ub at the bottom and Ut at the top, as well as the bottom plate, to fix the carbon fiber. Prior to molding of the specimen, the inside surface of the mold was coated with mineral oil or grease to allow carbon fibers to be easily removed without damage when being demolded. The production of specimens begins first with fixing bottom Ub on the bottom plate. Next, the carbon fiber is accurately placed on Ub. At this time, the carbon fiber must be wide enough not to get scattered even when the cement paste is poured. To ensure that the upper Ut, the lower Ub, and the carbon fiber in the middle are kept firmly engaged with one another, they are attached using double-sided tapes or rubber rings. Then, the cement paste is divided into two layers of the same thickness and carefully poured into the space between carbon fibers. Then, they are vibrated so that the cement paste around the carbon fiber is evenly distributed. When vibrating, special care should be

Table 2: Physical properties of the carbon fiber.

Filament diameter (μm)	Density (g/cm^3)	Tensile strength (MPa)	Elastic modulus (GPa)	Elongation (%)	Carbon content (wt.%)
7 ± 2	1.8	4,900	230	2.1	92

(a) (b)

Figure 5: Carbon fibers used in the experiment. (a) Nano-SiO_2-coated carbon fiber. (b) Plain carbon fiber.

Table 3: Description of fabrication of specimens for the pull-out test.

Type of cement pastes	Specimens	Replacement ratio of SF (wt.%)	Number of specimens	Remarks
PCF	PCFSF0-3 d	—	5	Cement paste prepared by using 100% cement and without SF at 3, 7, and 28 days
	PCFSF0-7 d		5	
	PCFSF0-28 d		5	
CCF	CCFSF0-3 d	—	5	
	CCFSF0-7 d		5	
	CCFSF0-28 d		5	
PCF	PCFSF10-3 d	10	5	Cement paste prepared by using 90% cement and with 10 wt.% SF at 3, 7, and 28 days
	PCFSF10-7 d		5	
	PCFSF10-28 d		5	
CCF	CCFSF10-3 d	10	5	
	CCFSF10-7 d		5	
	CCFSF10-28 d		5	

PCF is the plain carbon fiber; CCF is the nano-SiO_2-coated carbon fiber.

taken to make sure that carbon fibers do not move or do not change the direction. A total of 60 cubes ($40 \times 40 \times 40$ mm) of CFRCP specimens were completed for each test variable in this study in order to review the pull-out resistance performance of carbon fibers embedded in the cement paste matrix.

3. Results and Discussion

3.1. Morphology of the Carbon Fiber Surface Modified with a Nano-SiO_2 Particle. Figure 7 shows a photograph of the carbon fiber surface modified with a nano-SiO_2 particle and observed by SEM. Figure 7(a) is a plain carbon fiber,

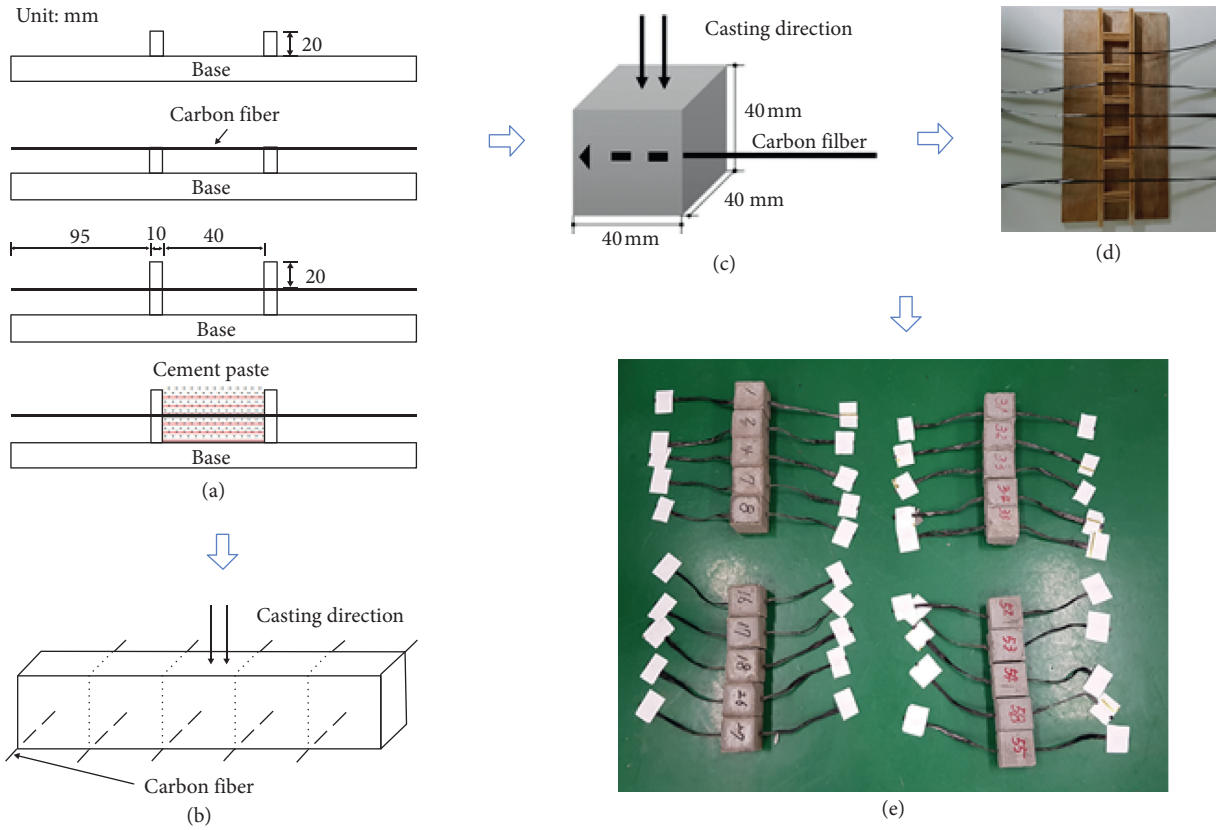

Figure 6: Schematic diagram of the production progress of each step for fabrication specimens of the carbon fiber.

Figure 7(b) is a carbon fiber pretreated with nitric acid, and Figure 7(c) is a photograph showing the carbon fiber coated with a nano-SiO_2 particle, observed by SEM, respectively. Compared to the plain carbon fiber in Figure 7(a), the carbon fiber pretreated with nitric acid of Figure 7(b) features a string in the axial direction, thereby increasing the surface roughness of the carbon fiber. The pretreatment of nitric acid in Figure 7(b) aims to intensify the surface roughness of the carbon fiber as well as to increase the number of COOH or OH functional groups on the surface of the carbon fiber through an oxidation reaction to easily attach nano-SiO_2 particles on its surface. From Figure 7(c) which shows the surface of carbon fiber coated with nano-SiO2 particles, it could be confirmed that nano-SiO_2 particles are uniformly dispersed on the surface of the carbon fiber.

3.2. Chemical Composition Analysis. SEM images were taken to confirm the morphology of the carbon fiber in the cement paste matrix, and the content of components on the surface of the carbon fiber (C, O, Si, Ca, etc.) was obtained by EDS analysis. As a measurement method, in order to accurately measure the elemental content, the content of elements was measured by obtaining the average value using a point-scanning method with a distance of 5 points equal to each carbon fiber. The detailed data are shown in Table 4. According to the analysis, carbon elements only remained on the surface of the plain carbon fiber that was not subjected to the coating process; meanwhile, the oxygen content increased slightly by about 2.51%. Although the oxygen content increased by 5.59% on the surface of the plain carbon fiber where silica fume was replaced by 10 wt.%, the carbon fiber content without the coating process was 94.41%. No other elements were found. On the surface of the carbon fiber modified with a nano-SiO_2 particle without silica fume, however, the contents of oxygen, silica, and calcium increased to 24.80%, 0.83%, and 2.79%, respectively, but the carbon content decreased to 27.56%. In other words, the silica and calcium contents increased slightly, while the oxygen content increased significantly. The contents of oxygen, silica, and calcium, which were replaced by 10 wt.% of silica fume and surface modified with a nano-SiO_2 particle, increased to 30.7%, 4.32%, and 7.99%, respectively, whereas the carbon content decreased drastically to 42.08%. From this, it is made known that the surface of the carbon fiber was coated with a large content of nano-SiO_2 particles because the nano-SiO_2 particles in the cement paste matrix reacted with Ca $(OH)_2$, generating C-S-H gel and the like. Owing to the reaction of $Ca(OH)_2$ like this, large contents of oxygen and silica, as well as calcium, elements were detected in a thin layer of hydration products covering the surface of the carbon fiber. This is because a thin layer of nano-SiO_2 particles coated on the surface of modified carbon fibers reacted with $Ca(OH)_2$, which induced formation of a cement hydration product through creation of C-S-H gel.

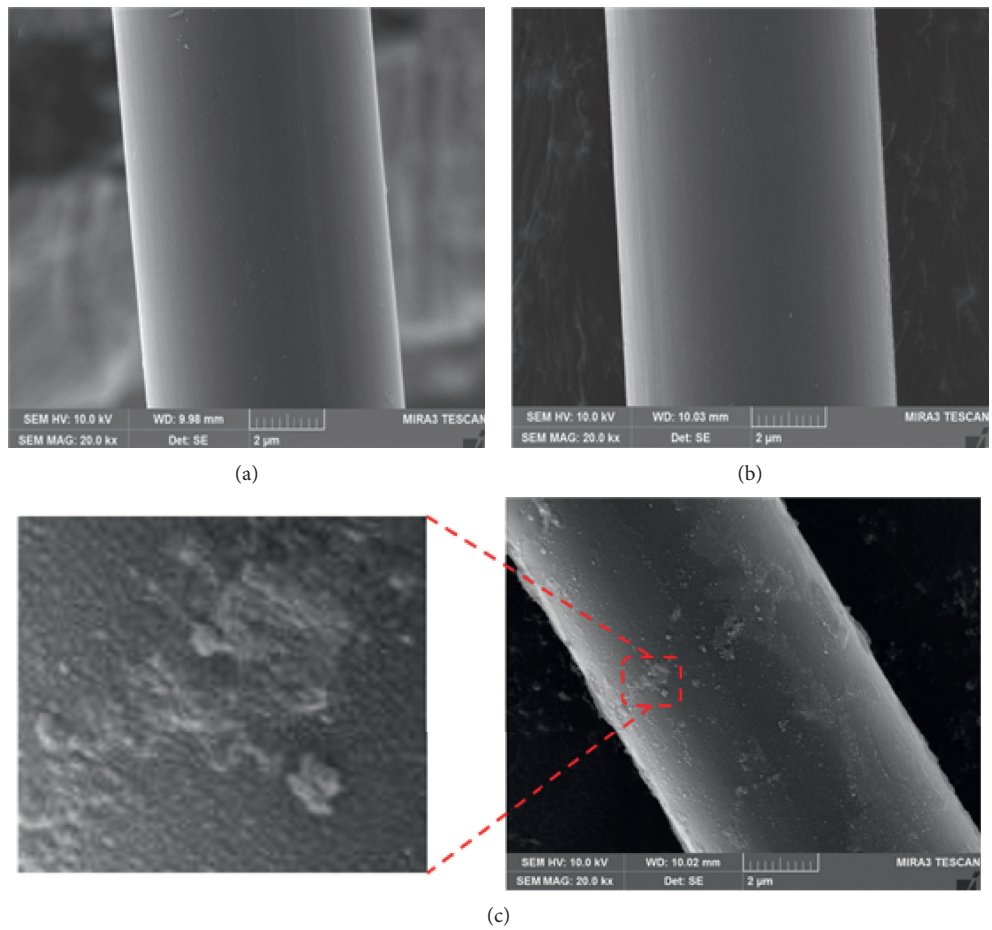

Figure 7: Surface topography of the carbon fiber (20,000x). (a) Plain carbon fiber. (b) Nitric acid-treated carbon fiber. (c) Nano-SiO_2-coated carbon fiber.

Table 4: Element analysis results of the carbon fiber surface.

Carbon fiber in the cement paste matrix	Element content (%)							
	C	O	Si	Ca	Mg	Al	S	K
Plain carbon fiber without SF	97.49	2.51	—	—	—	—	—	—
Plain carbon fiber with 10 wt.% SF	94.41	5.59	—	—	—	—	—	—
Nano-SiO_2-coated carbon fiber without SF	69.93	24.80	0.83	2.79	1.2	0.19	0.10	0.16
Nano-SiO_2-coated carbon fiber with 10 wt.% SF	55.41	30.7	4.32	7.99	0.36	0.64	0.33	0.25

3.3. FT-IR Spectrum Analysis. Figure 8 shows the results of FT-IR spectrum analysis for the chemical structure of the plain carbon fiber (Figure 8(a)), a nano-SiO_2-coated carbon fiber (Figure 8(b)), and C-S-H gel carbon fiber obtained by reacting with $Ca(OH)_2$ (Figure 8(c)). It can be seen from Figure 8 that compared to the plain carbon fiber of Figure 8(a), the nano-SiO_2-coated carbon fiber in Figure 8(b) has a strong absorption peak due to the Si-O-Si stretching vibration at 1040 cm^{-1}, confirming that nano-SiO_2 particles are attached to the carbon fiber. Figure 8(c) shows the carbon fiber in the cement paste matrix and confirms that an absorption peak of the C-O stretching vibration was generated at 1437 cm^{-1}. This may serve as the basis for confirming that C-S-H gel is produced as C-O in calcium carbonate created by the reaction of C-S-H gel with carbon dioxide (CO_2) in the atmosphere. Furthermore, it is believed that the nano-SiO_2 particles attached to the surface of the carbon fiber are fully cultivated, and thus, its hydrophilicity has increased. In case of the plain carbon fiber, however, it can be seen that the stretching vibration cannot be formed at 1040 cm^{-1} and 1437 cm^{-1}.

3.4. Compressive Strength Test Results. The compressive strength test of the cement paste specimens was determined by the average values of three specimens at 28 days of age. As a result of the compression test, the compressive strength of the plain cement paste was 36.6 MPa. Meanwhile, the

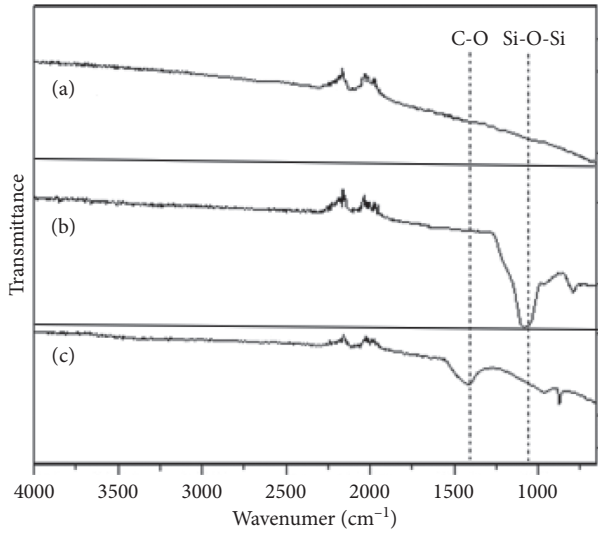

Figure 8: FT-IR spectrum of carbon fiber surface modified with different methods. (a) Plain carbon fiber. (b) Nano-SiO_2-coated carbon fiber. (c) C-S-H gel carbon fiber.

compressive strength of the cement pastes with 10 wt.% of silica fume was 39.4 MPa. Compared to the plain cement paste, it was found that the compressive strength increased by about 7.7%.

3.5. Pull-Out Test Results

3.5.1. Pull-Out Resistance Performance. This study refers to the results of existing researchers because no clear standard regulation has yet been proposed for the method of pulled-out fibers in the cement matrix [47–49]. The interfacial bond performance between the fiber and the matrix is very closely related to the performance of FRCC, and the surface morphology, physical properties, matrix strength, etc. of the fiber play an extremely important role in the interfacial bond performance between the fiber and the matrix. The bond properties of these fibers are directly connected with the effect of increasing the interfacial bonding force of the cement composite material and have also a vast influence on the flexural and pull-out behaviors of FRCC. In this study, pull-out tests were conducted at 3, 7, and 28 days of age, respectively, to review the pull-out resistance performance of CFRCP specimens. With respect to the specimens of the cement paste ($40 \times 40 \times 40$ mm) for each test variable, the displacement and frictional bond strength at the maximum load by the pull-out tests were compared and analyzed. The results on the pull-out test of specimens are summarized in Table 5. To secure the validity of the test results, the maximum/minimum values of 5 identical specimens were excluded, and the average values were calculated from 3 specimens. According to the data obtained from Table 5, the range of standard deviation for frictional bond strength is about 0.07 to 0.81 in case of the plain carbon fiber specimens but is about 0.21 to 1.01 in case of the carbon fiber specimens coated with a nano-SiO_2 particle. Thus, it can be seen from the above data that the dispersion degree of the standard deviation is larger than that of the plain carbon fiber specimens. Meanwhile, Figure 9 is a photograph of the state of measurement using an electronic scale for calculating the diameter of the tow carbon fiber. When the length of the carbon fiber is 10 m, the mass value measured with an electronic balance is 7.21 g which was used to calculate the nominal diameter of the bundle-form tow carbon fiber. At this time, the mass of the carbon fiber corresponds to 1.8 g/cm^3. For the calculation of frictional bond strength, the diameter of the bundle-shaped tow carbon fiber was about 0.714 mm. Figure 10 shows the variation in frictional bond strength according to the age of the plain carbon fiber specimens and the carbon fiber specimens coated with a nano-SiO_2 particle depending on with or without silica fume, the data for which are obtained from the pull-out tests. As shown in Figure 10(a), in the case of the plain carbon fiber specimens without silica fume, frictional bond strength was 3.90 MPa, 4.06 MPa, and 4.42 MPa at 3, 7, and 28 days of age, respectively. It showed a tendency to increase slightly. On the contrary, the frictional bond strength of the carbon fiber specimens coated with a nano-SiO_2 particle was somewhat increased to 4.77 MPa, 5.14 MPa, and 5.63 MPa, respectively. Compared to the plain carbon fiber specimens, the frictional bond strength of the carbon fiber specimens coated with a nano-SiO_2 particle increased by about 0.87 MPa, 1.08 MPa, and 1.21 MPa, respectively, proving improvement of the pull-out resistance performance by about 22.3%, 26.6%, and 27.3%, respectively. Meanwhile, as shown in Figure 10(b), in the case of the plain carbon fiber specimens with silica fume replaced by 10 wt.%, frictional bond strength was 4.29 MPa, 4.38 MPa, and 4.36 MPa at 3, 7, and 28 days of age, respectively. It showed a tendency to be similar. On the contrary, the frictional bond strength of the carbon fiber specimens coated with a nano-SiO_2 particle was somewhat increased to 5.24 MPa, 5.39 MPa, and 5.80 MPa, respectively. Compared to the plain carbon fiber specimens, the frictional bond strength of the carbon fiber specimens coated with a nano-SiO_2 particle increased by about 0.95 MPa, 1.01 MPa, and 1.44 MPa, respectively, proving improvement of the pull-out resistance performance by about 22.1%, 23.0%, and

Table 5: Obtained results from the pull-out test.

Type of specimens	Replacement ratio of SF (wt.%)	No. of specimens	Maximum load (N)	Displacement at max. load (mm)	Frictional bond strength (sd)	
					τ_{max} (MPa)	Ratio (B/A, %)
PCFSF0-3 d (A)	—	1	283	2.48	3.15	122.3
		2	380	2.60	4.23	
		3	387	3.05	4.31	
		Average	350	2.71	3.90 (0.65)	
CCFSF0-3 d (B)		1	486	3.15	5.41	
		2	475	2.67	5.29	
		3	324	2.35	3.61	
		Average	428	2.72	4.77 (1.01)	
PCFSF0-7 d (A)		1	361	2.76	4.02	126.6
		2	372	1.89	4.14	
		3	362	1.90	4.03	
		Average	365	2.18	4.06 (0.07)	
CCFSF0-7 d (B)		1	424	2.54	4.72	
		2	487	2.61	5.29	
		3	475	2.67	5.42	
		Average	462	2.60	5.14 (0.37)	
PCFSF0-28 d (A)		1	325	2.52	3.62	127.3
		2	471	2.56	5.24	
		3	394	2.55	4.39	
		Average	397	2.54	4.42 (0.81)	
CCFSF0-28 d (B)		1	484	2.68	5.39	
		2	514	3.13	5.72	
		3	520	2.29	5.79	
		Average	506	2.70	5.63 (0.21)	
PCFSF10-3 d (A)	10	1	414	1.80	4.61	122.1
		2	355	2.32	3.95	
		3	387	3.05	4.31	
		Average	385	2.39	4.29 (0.33)	
CCFSF10-3 d (B)		1	501	3.15	5.58	
		2	450	3.44	5.01	
		3	461	3.23	5.13	
		Average	471	3.27	5.24 (0.30)	
PCFSF10-7 d (A)		1	412	2.08	4.59	123.0
		2	352	2.98	3.92	
		3	416	3.28	4.63	
		Average	393	2.78	4.38 (0.40)	
CCFSF10-7 d (B)		1	481	2.54	5.36	
		2	509	3.30	5.67	
		3	463	2.87	5.15	
		Average	484	2.90	5.39 (0.26)	
PCFSF10-28 d (A)		1	421	2.53	4.69	133.0
		2	354	2.32	3.94	
		3	401	2.50	4.46	
		Average	392	2.45	4.36 (0.38)	
CCFSF10-28 d (B)		1	579	2.87	6.45	
		2	529	2.82	5.89	
		3	456	2.93	5.08	
		Average	521	2.87	5.80 (0.69)	

sd is the standard deviation; B/A is the increase ratio of frictional bond strength.

Figure 9: Electronic scale for the calculation of the diameter of the tow carbon fiber.

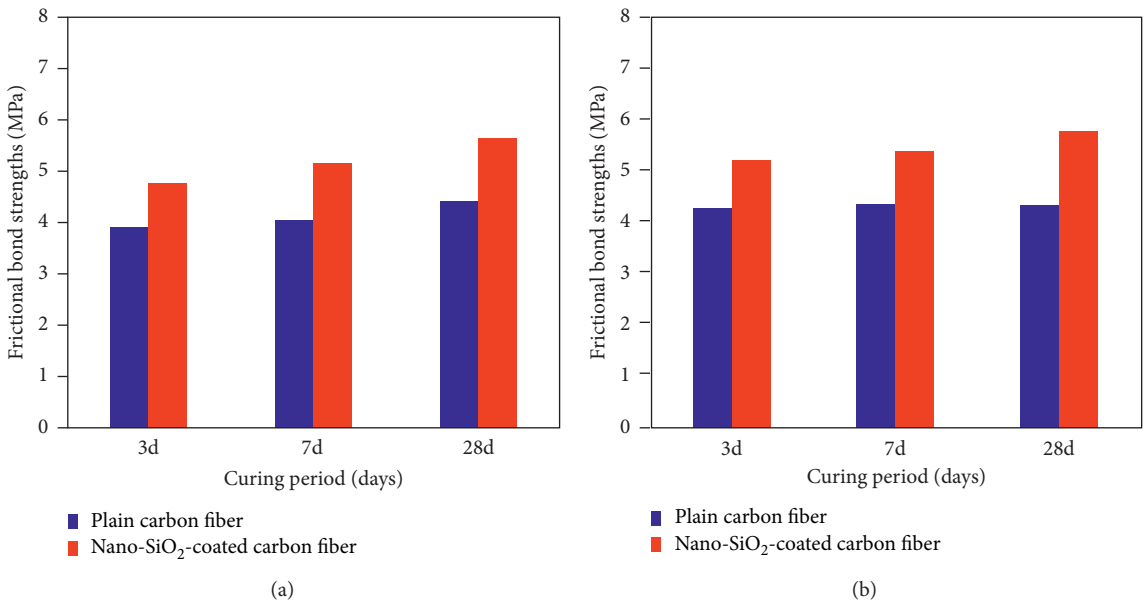

Figure 10: Variation of frictional bond strength at 3, 7, and 28 days of age. (a) Carbon fiber without SF. (b) Carbon fiber with 10 wt.% SF.

33.0%, respectively. Therefore, the frictional bond strength at the maximum load in the interface is in the order of CCFSF10 〉 CCFSF0 〉 PCFSF10 〉 PCFSF0 specimens, signifying that the CCFSF10 specimen has the highest pull-out resistance performance, while the PCFSF0 specimen owns relatively the lowest one. This shows that the frictional bond strength between the carbon fiber and the cement paste matrix increased due to the effect of increasing the interfacial bonding force of the carbon fiber specimens coated with a nano-SiO_2 particle. In particular, it can be seen that when silica fume is incorporated into carbon fibers coated with a nano-SiO_2 particle, it is more advantageous to secure a pull-out resistance performance.

3.5.2. Pull-Out Stress-Displacement Curves. Figure 11 shows the stress-displacement curve relationship obtained from the pull-out tests for a group of the CFRCP specimens (three specimens) without silica fume. As seen in Figure 11, the maximum frictional bond strength of the plain CFRCP specimens was about 3.15–5.24 MPa at 3, 7, and 28 days of age, whereas the maximum frictional bond strength of the

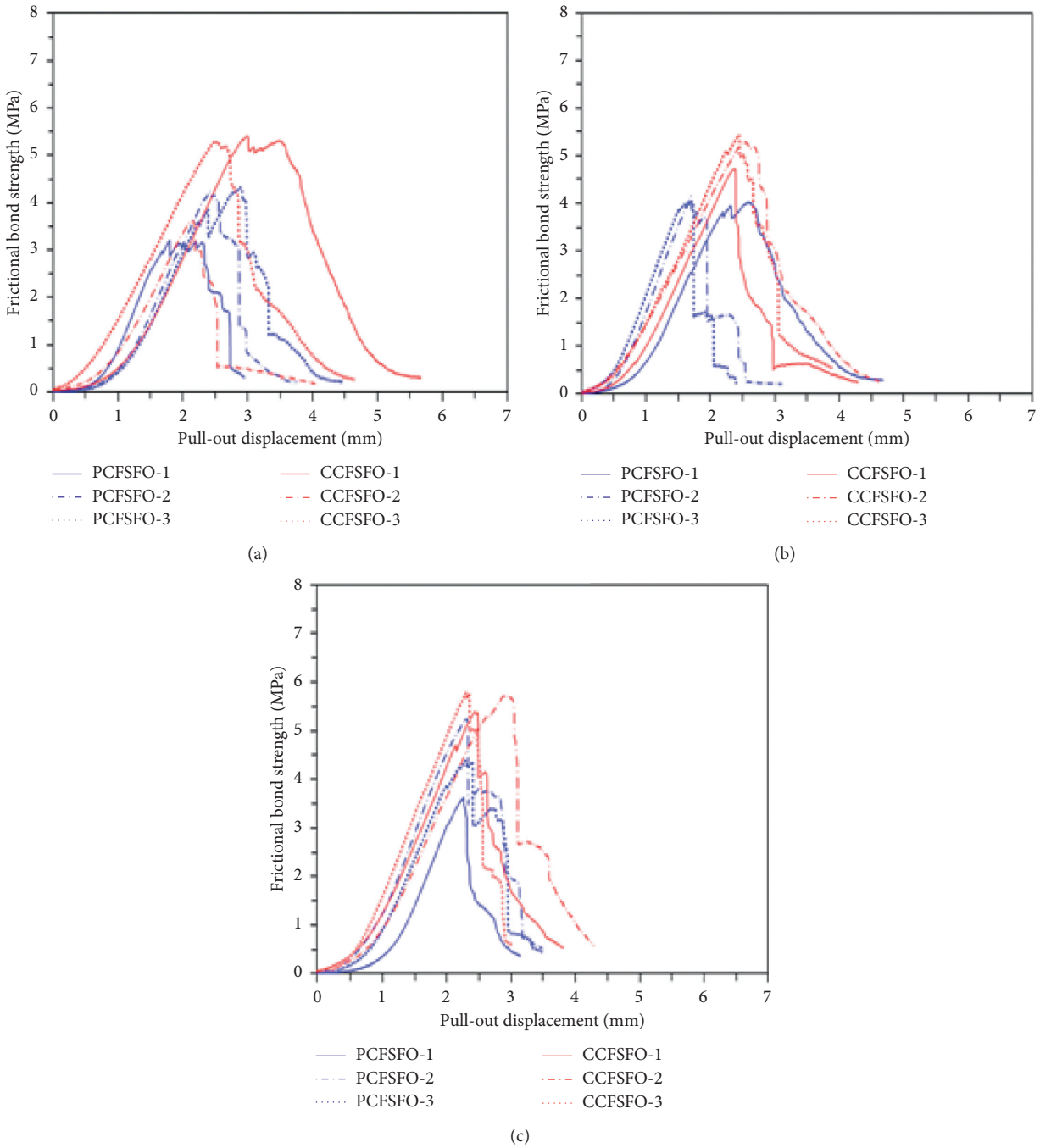

Figure 11: Stress-displacement curves of the pull-out test for the specimens without SF. (a) 3 d. (b) 7 d. (c) 28 d.

CFRCP specimens coated with a nano-SiO_2 particle was about 3.61–5.79 MPa, which showed a tendency to increase slightly with increasing age compared to the plain CFRCP specimens. Figure 12 shows the stress-displacement curve relationship obtained from the pull-out tests for a group of the CFRCP specimens (three specimens) with 10 wt.% silica fume. As seen in Figure 12, the maximum frictional bond strength of the plain CFRCP specimens was about 3.92–4.69 MPa at 3, 7, and 28 days of age, whereas the maximum frictional bond strength of the CFRCP specimens coated with a nano-SiO_2 particle was about 5.01–6.45 MPa, which showed a tendency to increase fairly with increasing age compared to the plain CFRCP specimens. Whether with silica fume or not, the pull-out stress of the fiber increased linearly in the initial stage, and then the pull-out stress-displacement behavior changed to nonlinearity, thus reaching the maximum bond strength. The curve of the plain CFRCP specimens showed a pull-out behavior in which the descending slop gradually decreased after the maximum bond strength, and the stress typically exhibited no sudden drops. On the contrary, the CFRCP specimens coated with a nano-SiO_2 particle showed almost the same pull-out

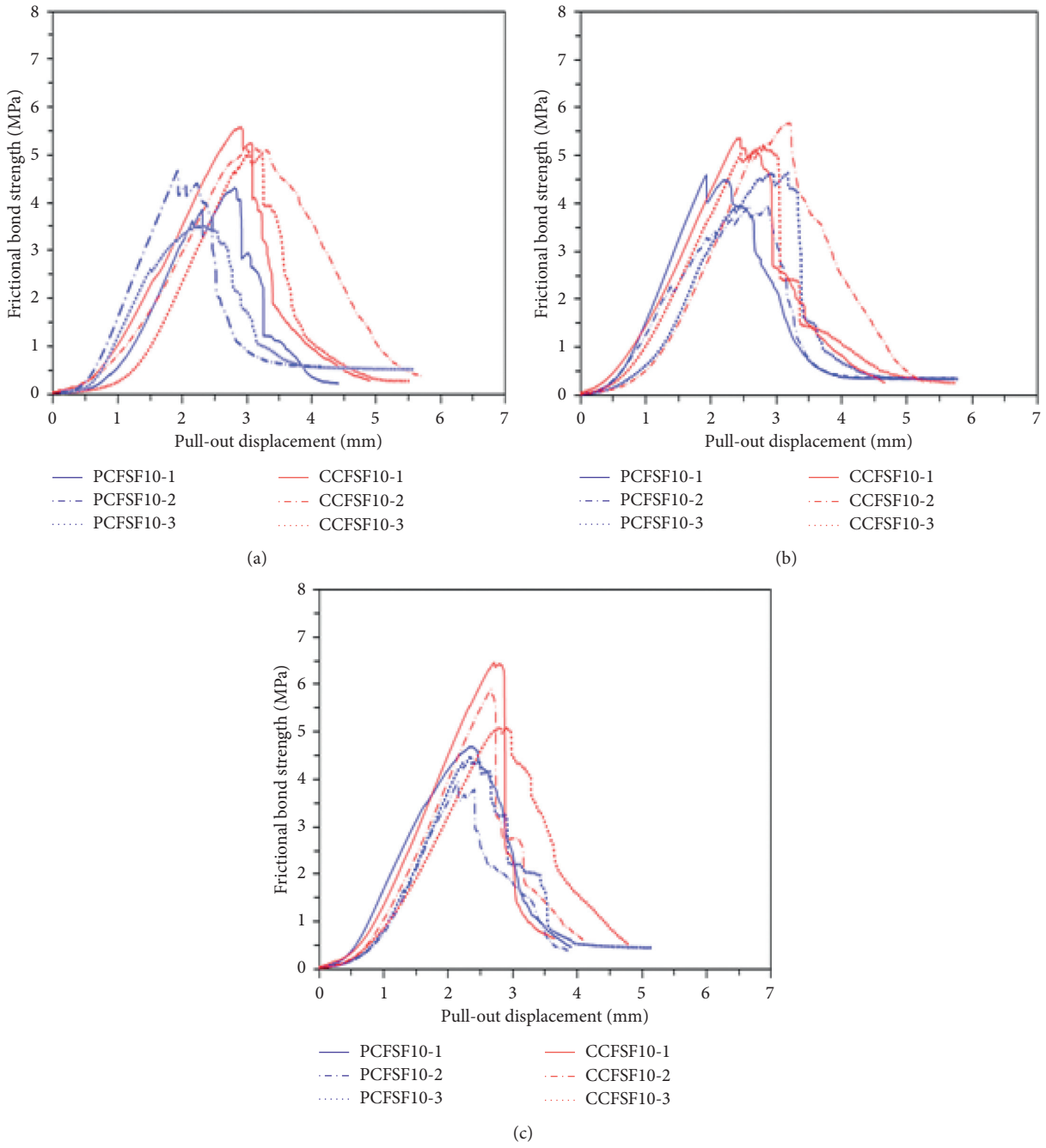

Figure 12: Stress-displacement curves of the pull-out test for the specimens with 10 wt.% SF. (a) 3 d. (b) 7 d. (c) 28 d.

behavior as the plain CFRCP specimens, but the pull-out behavior rapidly decreased after the maximum bond strength. This is because the plain CFRCP specimens have little chemical bond between the fibers and the matrix, whereas a chemical bond does occur between the fibers and the matrix of the CFRCP specimens coated with nano-SiO_2. As the stress continues to increase, the curve for CFRCP specimens coated with a nano-SiO_2 particle exhibits similar behavior to that for the plain CFRCP specimens, but the maximum value remains higher than that for the plain CFRCP specimens. Therefore, as regards the difference in the pull-out behavior depending on whether the fiber is coated or uncoated, the CFRCP specimens coated with a nano-SiO_2 particle showed the slip-softening behavior with the increase in displacement after the maximum bond strength. It was found that the ability to maintain the stress was higher due to the adhesive force between the fibers and the matrix, and thus, the ductility was significantly improved. As a result, it can be seen that the frictional bond strength of the CFRCP specimens coated with a nano-SiO_2 particle was significantly improved due to the effect of increasing the interfacial bonding force.

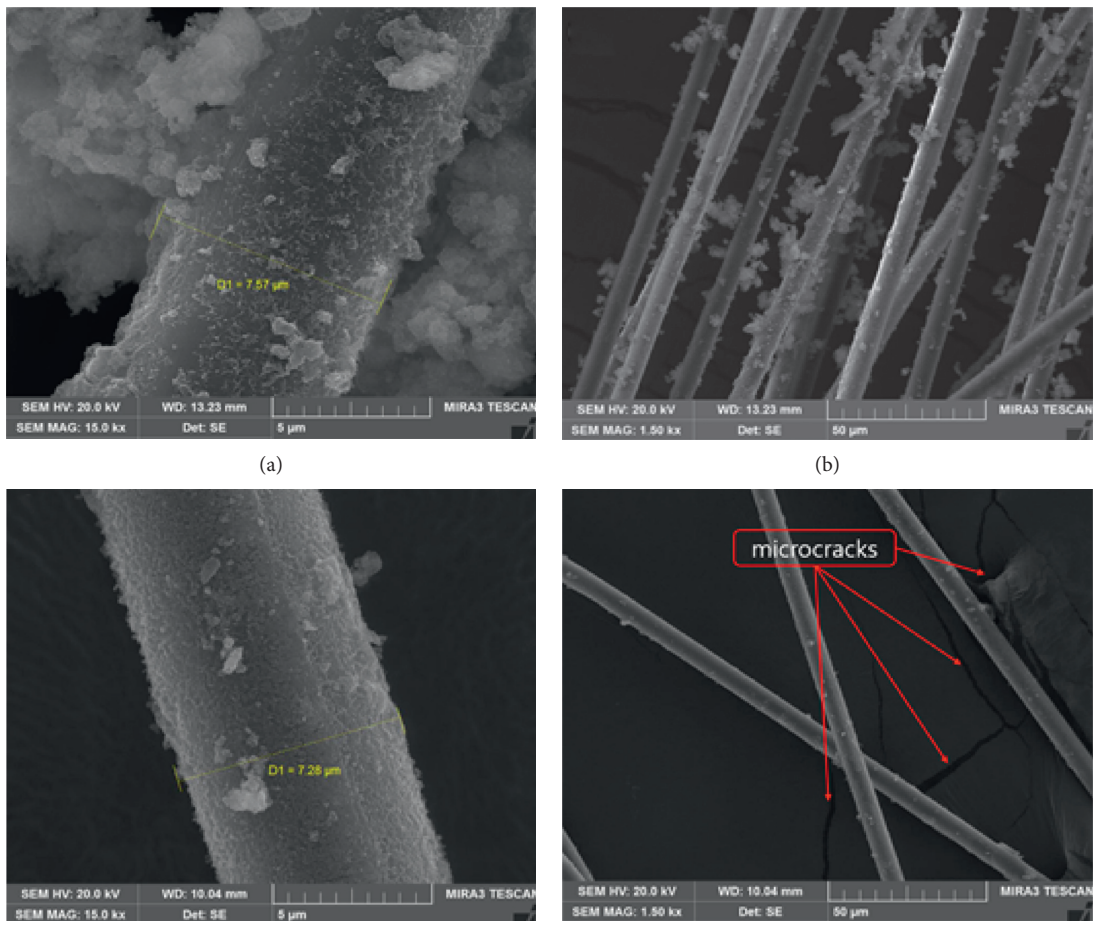

Figure 13: SEM images of the carbon fiber in the cement paste matrix after the pull-out test (15,000 or 1,500x). (a, b) Nano-SiO_2-coated carbon fiber with 10 wt.% SF. (c, d) Nano-SiO_2-coated carbon fiber without SF.

3.6. SEM Observation. Figures 13 and 14 show a photograph obtained through SEM observation of the cross section where fracture occurred in the carbon fiber taken from the specimen after the pull-out test conducted to confirm the interfacial bonding force of CFRCP specimens. SEM images of the surface morphology of the carbon fibers at magnifications of 15,000x and 1,500x are shown in Figures 13 and 14. In general, it has been reported that the thickness between the fiber and the cement matrix interface is about 20~100 μm, and this interface thickness has a great influence on strength and durability associated with cracking [50]. As seen in Figures 13(a) and 13(b), it could be confirmed that, in case of the carbon fiber coated with a nano-SiO_2 particle with 10 wt.% of silica fume, small and large particles in size of tens of nanometers are distributed fairly and uniformly on the surface of the carbon fiber, but microcracks and pores hardly appeared. Based on this, it can be seen that the interfacial bonding force between the fiber and the cement matrix is improved. Here, the surface of the carbon fiber was wrapped with a thin layer and became thicker with the surrounding hydration material. This seems to hydrate the fine powder of silica fume between the hydrated cement pastes, and it seems that the fine powder of silica fume is being progressed to promote a hydration reaction more actively. The diameter was about 7.57 μm as seen in Figure 13(a). During the hydration process, some of the hydrated materials "depart" the cement particles, resulting in some "gaps" between the fibers and the hydrated cement paste. SEM image shows a fairly wide range of hydrated substances in a dense form and features them sporadically. From Figures 13(c) and 13(d), it can be seen that a few tens of nanometer-sized particles are bonded to the surface of the carbon fiber coated with a nano-SiO_2 particle and without silica fume. It showed that microcracks are occurring between the fiber and the cement matrix. It can be seen that a thin film layer of nano-SiO_2 particles coated on the surface of the modified carbon fiber reacted with $Ca(OH)_2$ to induce the expansion of the cement hydration product through the formation of a C-S-H gel. The diameter was about 7.28 μm as seen in Figure 13(c). As seen in Figures 14(a) and 14(b), it was observed that 10 wt.% of silica fume was replaced, and some silica fume particles and large content of hydrated substances existed in a cohesive state on the surface of the plain carbon fiber. It was confirmed here that microcracks or pores hardly appeared. The diameter was about 6.96 μm as seen in Figure 14(a). Figures 14(c) and 14(d) show that silica fume was not replaced, and in case of the plain carbon fiber, the shape of the fiber surface was still very clean

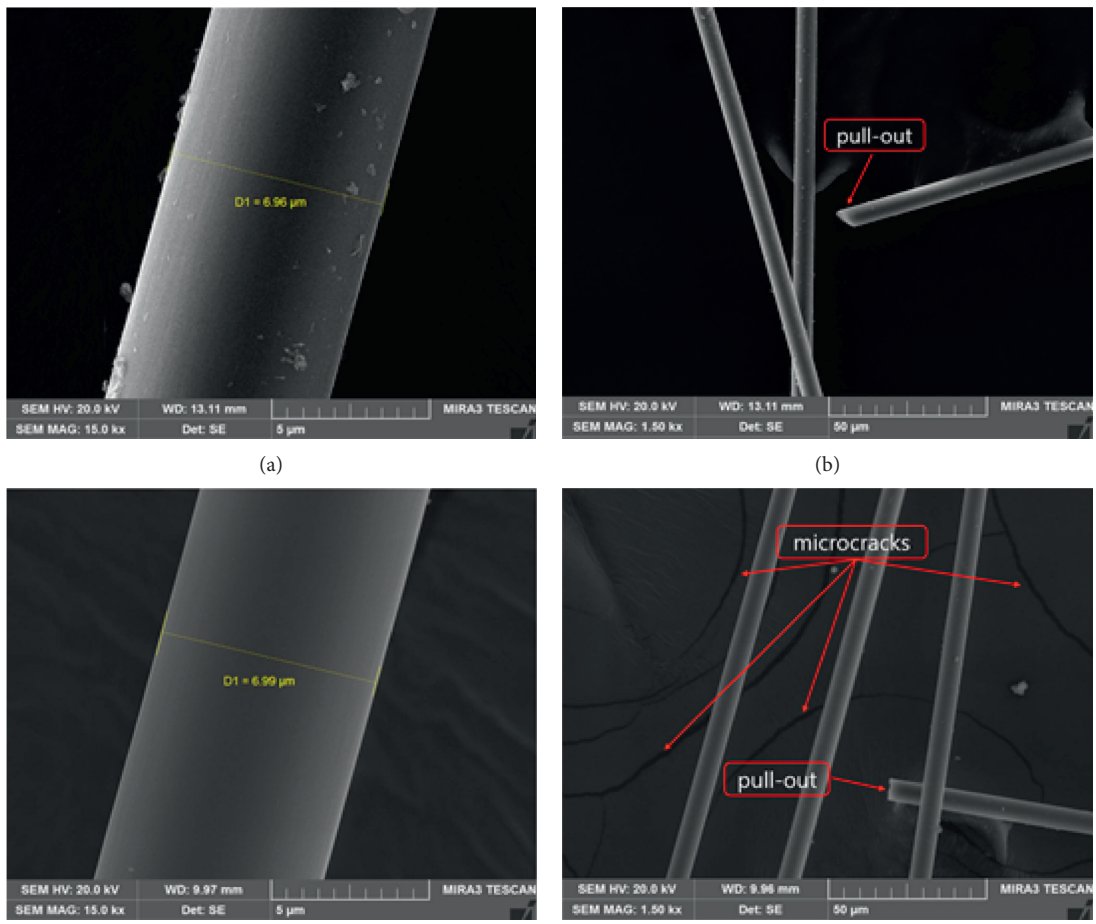

Figure 14: SEM images of the carbon fiber in the cement paste matrix after the pull-out test (15,000 or 1,500x). (a, b) Plain carbon fiber with 10 wt.% SF. (c, d) Plain carbon fiber without SF.

and fairly smooth. It can also be observed that microcracks frequently occur between the fiber and the matrix. The diameter was about 6.99 μm as seen in Figure 14(c). At this time, it is shown that the separation between the fiber and the cement matrix is occasionally occurring due to a pull-out phenomenon rather than fiber fracture due to insufficient strength and adhesion performance. This is confirmed to be attributable to the fact that the interfacial bonding force between the fiber and the matrix is low because the cement hydration product is difficult to crystallize, and as a result, the affinity gets lowered. Therefore, it can be seen from the SEM observation that the carbon fiber coated with a nano-SiO_2 particle has a higher interfacial bonding force than the plain carbon fiber because the formation of the secondary C-S-H gel on the fiber surface conduces in densification of the cement hydrate.

4. Conclusions

In this study, a method of effectively modifying the surface of carbon fibers with nano-SiO2 particles by chemical adhesion has been proposed to improve the interfacial bonding force between the fibers and the cement matrix as cement reinforcement materials. The surface morphology, chemical composition, and chemical structure of the carbon fiber surface modified with a nano-SiO_2 particle were analyzed using SEM, EDS, and FT-IR. The analysis results showed that a thin layer of nano-SiO_2 particles coated was uniformly distributed on the surface of the carbon fiber. A thin layer of coating is extremely dense, and its outermost is very rough. This is expected to improve the interfacial bonding force between the surface modified carbon fiber and the matrix. In addition, a pull-out test of tow carbon fibers embedded in the cement paste matrix was performed to review the interfacial bond properties of nano-SiO_2 particles produced on the surface of the carbon fiber. As a result of the pull-out test, it was confirmed that the carbon fiber coated with a nano-SiO_2 particle in the cement paste matrix had significantly improved the frictional bond strength compared to the plain carbon fiber, regardless of with and without replacement of silica fume. Compared to the plain carbon fiber, the frictional bond strength of the carbon fiber coated with a nano-SiO_2 particle increased by about 22.1–22.3%, 23.0–26.6%, and 27.3–33.0% at 3, 7, and 28 days of age, respectively. This may be because the chemical reaction occurred between nano-SiO_2 particles coated on the surface of the carbon fiber and $Ca(OH)_2$, resulting in improved chemical bonding

force. The new surface modification method of carbon fibers developed in this study is believed to greatly contribute to the development of fiber-reinforced cement-based composite materials.

Data Availability

The data used to support the findings of this study are available from the corresponding author upon request.

Conflicts of Interest

The authors declare that there are no conflicts of interest regarding the publication of this paper.

Acknowledgments

This research was supported by Basic Science Research Program through the National Research Foundation of Korea (NRF) funded by the Ministry of Education (Grant no. NRF-2018R1A6A1A03025542).

References

[1] M. Hambach and D. Volkmer, "Properties of 3D-printed fiber-reinforced portland cement paste," *Cement and Concrete Composites*, vol. 79, pp. 62–70, 2017.

[2] M. H. Beigi, J. Berenjian, O. Lotfi Omran, A. Sadeghi Nik, and I. M. Nikbin, "An experimental survey on combined effects of fibers and nanosilica on the mechanical, rheological, and durability properties of self-compacting concrete," *Materials & Design*, vol. 50, pp. 1019–1029, 2013.

[3] R. Liu, H. G. Xiao, H. Li et al., "Effects of nano-SiO_2 on the permeability-related properties of cement-based composites with different water/cement ratios," *Journal of Materials Science*, vol. 53, no. 7, pp. 4974–4986, 2018.

[4] S.-T. Kang, Y. Lee, Y.-D. Park, and J.-K. Kim, "Tensile fracture properties of an ultra high performance fiber reinforced concrete (UHPFRC) with steel fiber," *Composite Structures*, vol. 92, no. 1, pp. 61–71, 2010.

[5] D. j. Kim, A. E. Naaman, and S. EL-Tawil, "Comparative flexural behavior of four fiber reinforced cementitious composites," *Cement and Concrete Composites*, vol. 30, no. 10, pp. 917–928, 2008.

[6] K. Habel, E. Denarié, and E. Brühwiler, "Experimental investigation of composite ultra-high performance fiber-reinforced concrete and conventional concrete members," *ACI Structures Journal*, vol. 104, no. 1, pp. 93–101, 2006.

[7] Z. Rong, W. Sun, H. Xiao, and G. Jiang, "Effects of nano-SiO_2 particles on the mechanical and microstructural properties of ultra-high performance cementitious composites," *Cement and Concrete Composites*, vol. 56, pp. 25–31, 2015.

[8] A. M. Brandt, "Fibre reinforced cement-based (FRC) composites after over 40 years of development in building and civil engineering," *Composite Structures*, vol. 86, no. 1–3, pp. 3–9, 2008.

[9] K. Hannawi, H. Bian, W. Prince-Agbodjan, and B. Raghavan, "Effect of different types of fibers on the microstructure and the mechanical behavior of ultra-high performance fiber-reinforced concretes," *Composites Part B: Engineering*, vol. 86, pp. 214–220, 2016.

[10] M. H. Mobini, A. Khaloo, P. Hosseini, and A. Esrafili, "Mechanical properties of fiber-reinforced high-performance concrete incorporating pyrogenic nanosilica with different surface areas," *Construction and Building Materials*, vol. 101, pp. 130–140, 2015.

[11] V. Corinaldesi, A. Nardinocchi, and J. Donnini, "The influence of expansive agent on the performance of fibre reinforced cement-based composites," *Construction and Building Materials*, vol. 91, pp. 171–179, 2015.

[12] D.-Y. Yoo, J.-J. Park, S.-W. Kim, and Y.-S. Yoon, "Combined effect of expansive and shrinkage-reducing admixtures on the properties of ultra high performance fiber-reinforced concrete," *Journal of Composite Materials*, vol. 48, no. 16, pp. 1981–1991, 2014.

[13] G. H. Heo, J. G. Park, and C. G. Kim, "Evaluating the resistance performance of the VAEPC and the PAFRC composites against a low-velocity impact in varying temperature," *Advances in Civil Engineering*, vol. 2020, Article ID 7901512, 15 pages, 2020.

[14] R. Yu, P. Spiesz, and H. J. H. Brouwers, "Energy absorption capacity of a sustainable ultra-high performance fibre reinforced concrete (UHPFRC) in quasi-static mode and under high velocity projectile impact," *Cement and Concrete Composites*, vol. 68, pp. 109–122, 2016.

[15] V. Bindiganavile and N. Banthia, "Polymer and steel fiber-reinforced cementitious composites under impact loading-part 2: flexural toughness," *ACI Materials Journal*, vol. 98, no. 1, pp. 17–24, 2001.

[16] A. Bhutta, P. H. R. Borges, C. Zanotti, M. Farooq, and N. Banthia, "Flexural behavior of geopolymer composites reinforced with steel and polypropylene macro fibers," *Cement and Concrete Composites*, vol. 80, pp. 31–40, 2017.

[17] J.-P. Won, B.-T. Hong, T.-J. Choi, S.-J. Lee, and J.-W. Kang, "Flexural behaviour of amorphous micro-steel fibre-reinforced cement composites," *Composite Structures*, vol. 94, no. 4, pp. 1443–1449, 2012.

[18] G. A. Galhano, L. F. Valandro, R. M. de Melo, R. Scotti, and M. A. Bottino, "Evaluation of the flexural strength of carbon fiber-, quartz fiber-, and glass fiber-based posts," *Journal Endodontics*, vol. 31, no. 3, pp. 209–211, 2005.

[19] M. Hambach, H. Möller, T. Neumann, and D. Volkmer, "Portland cement paste with aligned carbon fibers exhibiting exceptionally high flexural strength (>100 MPa)," *Cement and Concrete Research*, vol. 89, pp. 80–86, 2016.

[20] J. Sun, F. Zhao, Y. Yao, X. Liu, Z. Jin, and Y. Huang, "A two-step method for high efficient and continuous carbon fiber treatment with enhanced fiber strength and interfacial adhesion," *Materials Letters*, vol. 196, no. 1, pp. 46–49, 2017.

[21] J. Sun, F. Zhao, Y. Yao, Z. Jin, X. Liu, and Y. Huang, "High efficient and continuous surface modification of carbon fibers with improved tensile strength and interfacial adhesion," *Applied Surface Science*, vol. 412, no. 1, pp. 424–435, 2017.

[22] W. Zemei, K. K. Henri, and S. Caijun, "Effect of nano-SiO_2 particles and curing time on development of fiber-matrix bond properties and microstructure of ultra-high strength concrete," *Cement Concrete Research*, vol. 95, pp. 247–256, 2017.

[23] C. Redon, V. C. Li, C. Wu, H. Hoshiro, T. Saito, and A. Ogawa, "Measuring and modifying interface properties of PVA fibers in ECC matrix," *Journal of Materials in Civil Engineering*, vol. 13, no. 6, pp. 399–406, 2001.

[24] J. Qiu, X.-N. Lim, and E.-H. Yang, "Fatigue-induced deterioration of the interface between micro-polyvinyl alcohol (PVA) fiber and cement matrix," *Cement and Concrete Research*, vol. 90, pp. 127–136, 2016.

[25] S. H. Kang, J. J. Kim, D. J. Kim, and Y.-S. Chung, "Effect of sand grain size and sand-to-cement ratio on the interfacial

bond strength of steel fibers embedded in mortars," *Construction and Building Materials*, vol. 47, pp. 1421–1430, 2013.

[26] G.-H. Heo, K.-C. Song, J.-G. Park, J.-H. Park, and H.-M. Jun, "Effect of mechanical properties of SiO_2 coated carbon fiber reinforced mortar composites," *Journal of the Korea Concrete Institute*, vol. 32, no. 1, pp. 65–76, 2020.

[27] B. Gao, R. Zhang, M. He et al., "Interfacial microstructure and mechanical properties of carbon fiber composites by fiber surface modification with poly(amidoamine)/polyhedral oligomeric silsesquioxane," *Composites Part A: Applied Science and Manufacturing*, vol. 90, pp. 653–661, 2016.

[28] H. Yao, X. Sui, Z. Zhao et al., "Optimization of interfacial microstructure and mechanical properties of carbon fiber/epoxy composites via carbon nanotube sizing," *Applied Surface Science*, vol. 347, pp. 583–590, 2015.

[29] T. Sugama, L. E. Kukacka, N. Carciello, and D. Stathopoulos, "Interfacial reactions between oxidized carbon fibers and cements," *Cement and Concrete Research*, vol. 19, no. 3, pp. 355–365, 1989.

[30] A. Bhutta, M. Farooq, C. Zanotti, and N. Banthia, "Pull-out behavior of different fibers in geopolymer mortars: effects of alkaline solution concentration and curing," *Materials and Structures*, vol. 50, no. 1, pp. 1–13, 2017.

[31] C. Sujivorakul, A. M. Waas, and A. E. Naaman, "Pullout response of a smooth fiber with an end anchorage," *Journal of Engineering Mechanics*, vol. 126, no. 9, pp. 986–993, 2000.

[32] D. L. Naik, A. Sharma, R. R. Chada, R. Kiran, and T. Sirotiak, "Modified pullout test for indirect characterization of natural fiber and cementitious matrix interface properties," *Construction and Building Materials*, vol. 208, pp. 381–393, 2019.

[33] J. M. Alwan, A. E. Naaman, and P. Guerrero, "Effect of mechanical clamping on the pull-out response of hooked steel fibers embedded in cementitious matrices," *Concrete Science and Engineering*, vol. 1, pp. 15–25, 1999.

[34] B. Koohestani, "Effect of saline admixtures on mechanical and microstructural properties of cementitious matrices containing tailings," *Construction and Building Materials*, vol. 156, pp. 1019–1027, 2017.

[35] H. Yan, W. Sun, and H. Chen, "The effect of silica fume and steel fiber on the dynamic mechanical performance of high-strength concrete," *Cement and Concrete Research*, vol. 29, no. 3, pp. 423–426, 1999.

[36] S. P. Cao, Q. F. Zhou, Y. L. Peng, and G. X. Li, "Effects of expansive agent and steel fiber on the properties of the fly ash ceramsite lightweight aggregate concrete," *Applied Mechanics and Materials*, vol. 357–360, pp. 1332–1336, 2013.

[37] Y.-W. Chan and S.-H. Chu, "Effect of silica fume on steel fiber bond characteristics in reactive powder concrete," *Cement and Concrete Research*, vol. 34, no. 7, pp. 1167–1172, 2004.

[38] Z. Wu, K. H. Khayat, and C. Shi, "Effect of nano-SiO_2 particles and curing time on development of fiber-matrix bond properties and microstructure of ultra-high strength concrete," *Cement and Concrete Research*, vol. 95, pp. 247–256, 2017.

[39] R. Kaur, N. C. Kothiyal, and H. Arora, "Studies on combined effect of superplasticizer modified graphene oxide and carbon nanotubes on the physico-mechanical strength and electrical resistivity of fly ash blended cement mortar," *Journal of Building Engineering*, vol. 30, pp. 1–12, 2020.

[40] X. Fu, W. Lu, and D. D. L. Chung, "Improving the tensile properties of carbon fiber reinforced cement by ozone treatment of the fiber," *Cement and Concrete Research*, vol. 26, no. 10, pp. 1485–1488, 1996.

[41] M. Lu, H. Xiao, M. Liu, X. Li, H. Li, and L. Sun, "Improved interfacial strength of SiO_2 coated carbon fiber in cement matrix," *Cement and Concrete Composites*, vol. 91, pp. 21–28, 2018.

[42] ASTM D 4018, *Standard Test Methods for Properties of Continuous Filament Carbon and Graphite Fiber tows*, American Standard for Testing and Materials, West Conshohocken, PA, USA, 2017.

[43] ASTM D 3039/D 3039M, *Standard Test Methods for Tensile Properties of Polymer Matrix Composite Materials*, American Standard for Testing and Materials, West Conshohocken, PA, USA, 2008.

[44] T. Kanda and V. C. Li, "Interface property and apparent strength of high-strength hydrophilic fiber in cement matrix," *Journal of Materials in Civil Engineering*, vol. 10, no. 1, pp. 5–13, 1998.

[45] KS F 2564, *Steel Fibers for Concrete*, Korean Standards Association, Seoul, South Korea, 2000.

[46] KS L ISO 679, *Methods of Testing Cements-Determination of Strength*, Korean Standards Association, Seoul, South Korea, 2016.

[47] L. Li, "Review interfacial characterization, control and modification of carbon fiber reinforced polymer composites," *Composites Science and Technology*, vol. 121, no. 16, pp. 56–72, 2015.

[48] V. C. Li and H. Stang, "Interface property characterization and strengthening mechanisms in fiber reinforced cement based composites," *Advanced Cement Based Materials*, vol. 6, no. 1, pp. 1–20, 1997.

[49] X. B. Zhang, H. Aljewifi, and J. Li, "Failure mechanism investigation of continuous fibre reinforced cementitious composites by pull-out behaviour analysis," *Procedia Materials Science*, vol. 3, pp. 1377–1382, 2014.

[50] K. L. Scrivener, A. K. Crumbie, and P. laugesen, "The interfacial transition zone (ITZ) between cement paste and aggregate in concrete," *Interface Science*, vol. 12, no. 4, pp. 411–421, 2004.